

Planetary Rover Exploration Combining Remote and In Situ Measurements for Active Spectroscopic Mapping

Alberto Candela¹, Suhit Kodgule¹, Kevin Edelson¹, Srinivasan Vijayarangan¹,
 David R. Thompson², Eldar Noe Dobrea³ and David Wettergreen¹

Abstract—Maintaining high levels of productivity for planetary rover missions is very difficult due to limited communication and heavy reliance on ground control. There is a need for autonomy that enables more adaptive and efficient actions based on real-time information. This paper presents an autonomous mapping and exploration approach for planetary rovers. We first describe a machine learning model that actively combines remote and rover measurements for mapping. We focus on spectroscopic data because they are commonly used to investigate surface composition. We then incorporate notions from information theory and non-myopic path planning to improve exploration productivity. Finally, we demonstrate the feasibility and successful performance of our approach via spectroscopic investigations of Cuprite, Nevada; a well-studied region of mineralogical and geological interest. We first perform a detailed analysis in simulations, and then validate those results with an actual rover in the field in Nevada.

I. INTRODUCTION

Mars rovers have accomplished important scientific and exploration objectives. However, it is challenging to keep high levels of productivity [1]. One of the main reasons is the heavy reliance on interaction between the rovers and ground operators, requiring substantial effort when planning and validating commands that are sent to the robots [2]. Furthermore, communication rate and bandwidth are limited. These factors result in additional days spent to accomplish mission objectives [1], [2].

Future missions would benefit from autonomous guidance of exploration. That is, a paradigm where the rover is guided by an evolving model of the explored environment, rather than a prescribed route. Such paradigm would enable rovers to take more adaptive and efficient actions based on real-time information, and ultimately improve mission productivity.

This paper presents a machine learning model that enables a rover to autonomously map a planetary surface. In order to achieve this goal, the model actively combines *remote* and *in situ* measurements. Remote sensing data collected by spacecraft such as the Mars Reconnaissance Orbiter (MRO) have been crucial in the large-scale understanding and mapping of Mars [3]. Unfortunately, these data often suffer from low resolution. Therefore, rovers are tasked with

¹A. Candela, S. Kodgule, K. Edelson, S. Vijayarangan and D. Wettergreen are with the Robotics Institute, Carnegie Mellon University, 5000 Forbes Avenue, Pittsburgh, PA 15213, USA {albertoc, skodgule, kedelson, svijayal, dsw0}@andrew.cmu.edu

²D. R. Thompson is with the Jet Propulsion Laboratory, California Institute of Technology, Pasadena, CA 91109, USA David.R.Thompson@jpl.nasa.gov

³E. Noe Dobrea is with the Planetary Science Institute, 1700 East Fort Lowell, Suite 106, Tucson, AZ 85719, USA eldar@psi.edu



Fig. 1. Zoë actively mapping and exploring at Cuprite, Nevada.

the collection of high-resolution *in situ* data that provide more definite results, but at smaller spatial scales. Naturally, the objective of our approach is to integrate both types of measurements *synergistically* to produce rich and dense maps. This work focuses on *spectroscopic mapping*. The reason is that spectroscopy has been critical for the study of surface composition and mineralogy on Mars, as well as its implications for climate and habitability [3], [4], [5], [6].

This work also derives an exploration strategy for improving mapping efficiency and productivity. We first incorporate notions from information theory, providing a quantitative basis that allows the robot to identify the most meaningful science measurements [7], [8], [9]. We then formulate rover exploration as an informative path planning problem that can be solved with many existing algorithms [10], [11], [12].

Finally, we demonstrate the feasibility and successful performance of our high-level autonomy approach via a case study. It involves spectroscopic investigations of Cuprite, Nevada; a well-studied region of mineralogical and geological interest concerning Earth [13], [14] and Mars [4], [5], [6]. We first perform a detailed analysis in simulations using real spectroscopic data. We then show field experiment results using Zoë (Figure 1), a rover developed at Carnegie Mellon University [15].

II. RELATED WORK

Robots have become excellent at detecting objects under static conditions, goals and assumptions [16], [17], [8], [18]. A few robots can go beyond detection to perform automatic science data analysis [19], [20], [21], [22]. However, they pursue static objectives that are fixed at the outset, such as detecting dust devils on Mars [23]. Some robots have used models based on Bayesian networks for mineral classification [18] or meteorite identification [17], but they also operate under predefined objectives that ignore the evolution of the robot's knowledge throughout the mission.

There are more adaptive models for autonomous robot exploration that rely on information-theoretic principles. Examples include Gaussian processes for binary terrain classification [8], ocean temperature mapping [20], [11] and plant phenotyping [24]. Nevertheless, they are limited to scalar field mapping and are unable to reconstruct high resolution data. Recent efforts have developed adaptive algorithms with high-level science objectives [9], [25]. However, they work with highly discretized models and fail to exploit valuable information that is available from remote sensing data.

We are especially interested in previous work that combines low (remote) and high (*in situ*) resolution data for robotic exploration. Thompson et al. presents a simple linear model that connects both, but actually downsamples the high resolution measurements and thus loses valuable information [26]. Candela et al. do the opposite by improving the details in low resolution data, but ignore important spatial correlations [27]. Foil and Wettergreen [28] and Thompson et al. [14] effectively utilize contextual information for surface classifications with spectroscopic data. However, informative robotic exploration needs a function to quantify and reward productivity, but in both cases it is either approximated [28] or ignored [14] due to computational difficulties.

III. ACTIVE SPECTROSCOPIC MAPPING

Planetary sciences rely on spectroscopic data for composition analysis. This is because each material reflects, emits, or absorbs light in a unique way throughout the wavelengths of the electromagnetic spectrum. The measured signals are called *spectra* and contain *features* that are used for rock and mineral identification [29]. Figure 2 shows an example of a *spectroscopic map*, a spatial structure where each coordinate is associated with a particular spectrum.

The paper focuses on the problem where a robotic explorer aims to learn the spatial distribution of spectra in the map or scene \mathcal{M} . We refer to this problem as *spatio-spectral regression*. We assume it can be done by combining two different types of measurements: low resolution *remote* spectra $x \in X \subset \mathbb{R}^m$, and high resolution *in situ* spectra $y \in Y \subset \mathbb{R}^n$. Remote spectra are available beforehand for many spatial locations $l \in L \subset \mathbb{R}^2$, whereas just a few *in situ* spectra can be collected by the rover in the field.

In order to solve this problem, we rely on *Gaussian process regression*, a machine learning method that has been widely used in spatial statistics [30] and informative robotic exploration [8], [20], [11], [24]. Nevertheless, previous

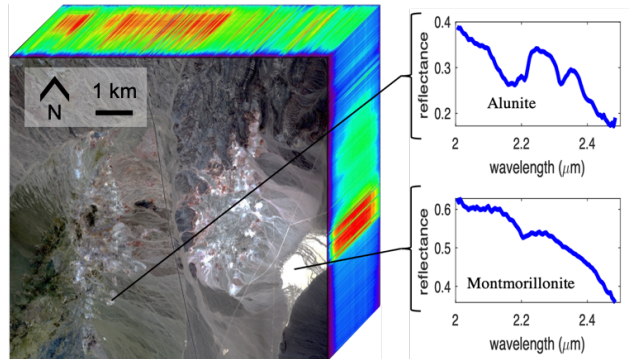


Fig. 2. A spectroscopic map of a 8×8 km area. Spectra are associated with each pixel and are used to identify specific minerals in the scene.

work focuses on mapping scalar fields such as temperature, whereas our goal is to learn high-resolution spectroscopic maps. In order to deal with this issue, we utilize *feature extraction* techniques, which reduce the dimensionality of the data by deriving a subset of non-redundant and informative features. The rest of this section describes how Gaussian process regression and feature extraction are used and combined in order to achieve the task of active spectroscopic mapping.

A. Feature Extraction

In situ spectroscopic measurements have high resolution. Many of these channels and wavelengths are highly correlated, allowing for the application of *dimensionality reduction* techniques. We use a variational autoencoder (VAE) [31], [32], a neural network that converts a set of high-resolution observations $y \in Y \subset \mathbb{R}^n$ into a set of lower dimensional features $z \in Z \subset \mathbb{R}^d$, where $d < n$. We specifically use a VAE because it learns a representation that resembles a standard multivariate normal distribution, i.e. $Z \sim \mathcal{N}_d(0, I_d)$, effectively normalizing and uncorrelating the features. The VAE is composed of two networks: an *encoder* that extracts the features, and a *decoder* that reconstructs high-resolution observations using the learned features. The architecture of the used VAE is similar to the one presented by Candela et al. [27]. It is important to underscore that the VAE ignores spatial information and correlations.

B. Gaussian Processes for Spatio-Spectral Regression

The robot uses a Gaussian process (GP) [33] for spatio-spectral regression, that is, to learn the spatial distribution of spectra throughout the scene. GPs are typically used for mapping scalar values, but our problem involves multivariate regression. We simplify by using GP regression to learn the distribution of low dimensional features Z instead. Moreover, dimensionality reduction with a VAE uncorrelates the learned feature representation, allowing for the utilization of d independent GPs.

We next provide a brief explanation regarding our specific GP regression model. If needed, extensive and canonical documentation can be found in [33]. Formally, we define an input vector that concatenates spatial coordinates and remote measurements as $v = [l, x] \in V \subset \mathbb{R}^{2+m}$, similarly as in [8].

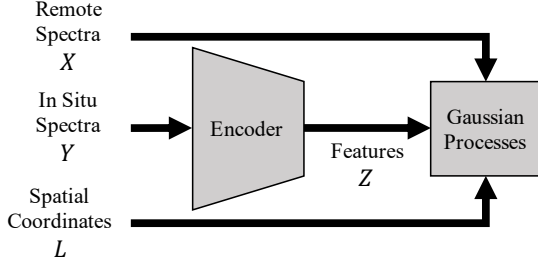


Fig. 3. The update step of the active spectroscopic mapping model.

We assume there exists a latent function $f^i : \mathbb{R}^{2+m} \rightarrow \mathbb{R}$ that maps an input v to each feature $z^i = f^i(v) + \epsilon_i$, where $i = 1, 2, \dots, d$. Each GP learns a distribution over the values that f^i can take. A GP is defined by a mean function μ^i and a covariance function K_θ^i , i.e. $f^i(v) \sim \mathcal{GP}(\mu^i(v), K_\theta^i(v, v'))$ [33]. We assume that the mean is zero because of the way features are normalized by the VAE. For the covariance matrix, we rely on the widely used *squared exponential kernel*. Similarly as in [8], we define an anisotropic kernel that distinguishes between spatial and spectral dimensions:

$$K_\theta^i(v, v') = \theta_0^i \exp\left(-\frac{\|l - l'\|_2^2}{2(\theta_l^i)^2} - \frac{\|x - x'\|_2^2}{2(\theta_x^i)^2}\right), \quad (1)$$

where $\theta^i = [\theta_0^i, \theta_l^i, \theta_x^i]$ are the kernel hyperparameters for each GP. Additionally, we utilize the GP variant for noisy observations, and thus use an additional hyperparameter σ_{noise}^i [33]. The GP hyperparameters are estimated by maximizing the log-likelihood of the observed data as shown in [33].

C. Active Spectroscopic Mapping Model

The active spectroscopic mapping model integrates feature extraction and GP regression. The learning process, as in Recursive Bayesian estimation, is composed of two steps: update and prediction [34]. In the update step (Figure 3), the learning model is improved when the robot collects *in situ* measurements. The d independent GPs are updated using the features that are extracted with the encoder of the VAE, along with the associated spatial coordinates and remote measurements. In the prediction step (Figure 4), the model uses this new knowledge in order to better reconstruct the scene. First, the GPs predict the features of each point $v \in V$ in the map using a normal distribution $\hat{Z} \sim \mathcal{N}(\hat{\mu}_Z(V), \hat{\Sigma}_Z(V))$ [33]. Then, these features are passed through the decoder of the VAE and reconstructed as high resolution spectra \hat{Y} .

IV. INFORMATIVE EXPLORATION

The rover aims to be efficient by collecting meaningful science measurements, that is, the ones that better explain and reconstruct the scene. Both in information theory and Bayesian experimental design, information-driven action selection can be formulated as the minimization of *posterior entropy*, which measures the uncertainty of a variable of interest after collecting new information [7], [9], [8], [24], [10]. In our scenario, the variable of interest is the spatial distribution of features throughout a spectroscopic map,

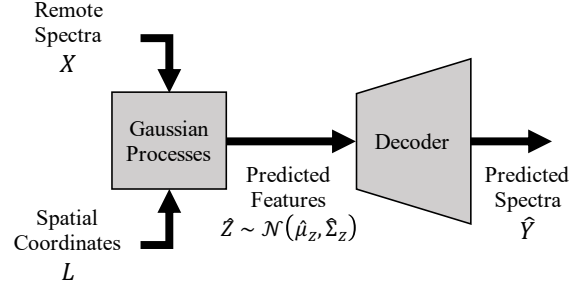


Fig. 4. The prediction step of the active spectroscopic mapping model.

which we assume is composed of a large, yet finite set of points $\mathcal{M} = \{v_1, \dots, v_p\}$. The new information is given by the *in situ* coordinates and measurements collected by the robot, i.e. $\mathcal{P} = \{[l_1, y_1], \dots, [l_k, y_k]\}$. The uncertainty of the model is quantified using Shannon entropy, which is additive for independent sources. Since the model consists of d independent GPs, the entropy of the map is additive for features and given by the following expression [7], [10]:

$$H(\mathcal{M}|\mathcal{P}) = \frac{1}{2} \sum_{i=1}^d \log \left((2\pi e)^{|\mathcal{M}|} |\hat{\Sigma}_{\mathcal{M}|\mathcal{P}}^i| \right), \quad (2)$$

where $\hat{\Sigma}_{\mathcal{M}|\mathcal{P}}^i$ is the predicted covariance of each feature z^i throughout the entire map \mathcal{M} after being updated with the *in situ* samples \mathcal{P} [33]. Then, an informative planner will attempt to solve an optimization problem where the robot's path should minimize the posterior entropy of the map:

$$\min_{\mathcal{P}} H(\mathcal{M}|\mathcal{P}) \quad \text{subject to} \quad \text{Cost}(\mathcal{P}) \leq \text{Budget}. \quad (3)$$

There exist many path planners that could be used for this problem, each with its own advantages and drawbacks. There are methods that assume independence between sampling locations, which is usually an oversimplification in informative exploration scenarios [35], [36]. There are also near-optimal greedy algorithms that work well on Gaussian processes [10], [24]. Other approaches may be computationally intensive, but potentially closer to optimality, such as branch and bound techniques for both discrete [11] and continuous [37] space representations. Finally, we are especially interested in Monte Carlo tree search (MCTS) planners that have been applied to geologic exploration scenarios [12], [25].

V. CASE STUDY

We demonstrate the feasibility and successful performance of our high-level autonomy approach in a case study. It involves spectroscopic investigations at Cuprite, Nevada; a well-studied region that is amenable to remote sensing and has a high mineralogical diversity [13], [14]. Furthermore, it is a region that has many of the minerals that have been found on Mars [5], [6]. We first perform a detailed analysis in simulations, and then show field results with a rover.

This study used data from three different spectrometers: the Advanced Spaceborne Thermal Emission and Reflection Radiometer (ASTER) [38], the Airborne Airborne Visible

TABLE I
MEASUREMENT AND INSTRUMENT SPECIFICATIONS

Instrument	Source	Used Wavelengths	Channels	Average Resolution
ASTER	Orbital	2.0 - 2.4 μm	5	80 nm
AVIRIS-NG	Airborne	2.0 - 2.4 μm	80	5 nm
ASD	Ground	2.0 - 2.4 μm	400	1 nm

Infrared Imaging Spectrometer Next Generation (AVIRIS-NG) [39], and an ASD FieldSpec Pro (ASD). ASTER is a low-resolution orbital instrument, AVIRIS-NG is a high-resolution airborne spectrometer, and ASD is a high-resolution *in situ* device. The data consisted of *reflectance spectra*, representing the fraction of incident light reflected in each wavelength. We restricted the models and analysis to the 2.0 - 2.4 μm infrared spectral region, as these wavelengths contain most of the diagnostic features needed for mineral identification at Cuprite [13]. Table I shows the wavelengths, channels, and resolutions that were used for each instrument. In the simulated experiments, ASTER provided remote measurements, whereas AVIRIS-NG served as the source of *in situ* measurements for both sampled and unsampled locations. In the field experiments, remote data also came from ASTER, but the rover collected *in situ* spectra with an onboard ASD instrument. Since ASD samples were sparse, AVIRIS-NG served as the ground truth.

We compare the performance of three planning algorithms:

- **Random**: sequentially samples a random neighboring location until the sampling budget is exhausted. This is a *science-blind* baseline.
- **Greedy**: sequentially samples the best neighboring location in hindsight using a one-step lookahead. This is a *myopic* exploration strategy.
- **MCTS**: the Monte Carlo tree-search planner by Kodgule et al. [12] using a four-step lookahead. This is a *non-myopic* path planner.

We use two metrics to evaluate the performance of the planners. The first one is the posterior *entropy* (Equation 2), which is *directly* minimized by the planners (Equation 3) and is calculated without a ground truth. The second one is the *reconstruction error* of the scene in terms of root mean squared error (RMSE). It should be *indirectly* minimized by the planners since it always requires a basis for comparison. For normalization purposes, we report the averages with respect to the total number of points in the map.

VI. SIMULATED EXPERIMENTS

A. Experimental Setup

We first perform an evaluation of the learning and exploration strategies through a simulation study. Three hundred different traverses were simulated using random starting locations. We defined a constraint of 20 samples per traverse. Additionally, a digital elevation model (DEM) from ASTER was used to apply a slope constraint of 18°. The ASTER and AVIRIS-NG data products were spatially aligned and resampled to a resolution of 15 m/pixel. We represented the

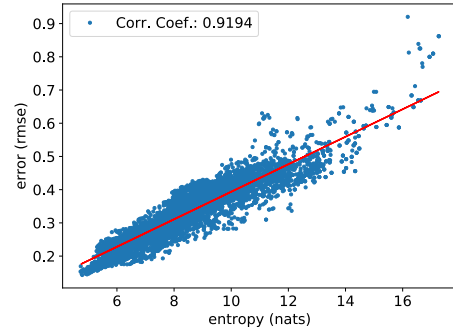


Fig. 5. Scatter plot for average reconstruction error and entropy.

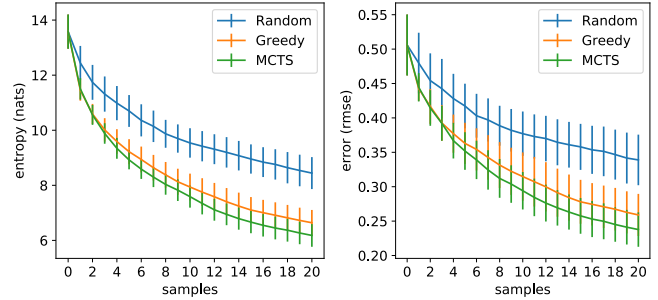


Fig. 6. Plots and 1-sigma error bars for entropy and reconstruction error as a function of collected samples per traverse (smaller is better).

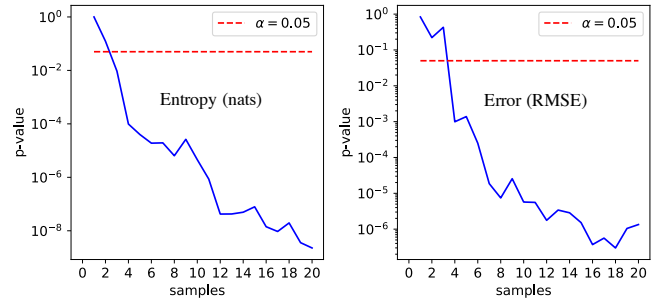


Fig. 7. Paired t-tests between the Greedy and MCTS planners. Points below the threshold indicate that MCTS performs better with a 95% confidence.

exploration space as an 8-connected grid using a pixel step size of 2. We focused on a 1 × 1 km subregion of Cuprite that is mineralogically diverse and relatively traversable.

Both the VAE and the GPs (Section III) were trained with a subset of the data that was withheld from the experiments. The VAE learned how to extract features from AVIRIS-NG spectra by encoding them into a space with dimensionality $d = 6$; a value we found to work well. The model consists of 6 independent GPs that were pre-trained with the same data set, and later fine-tuned online in order to better adapt to the incoming flow of data.

B. Results

We first analyze the correlation between entropy and reconstruction error throughout the simulations. Figure 5 shows a scatter plot with a correlation coefficient of 0.9194, indicating there exists a strong positive correlation. This

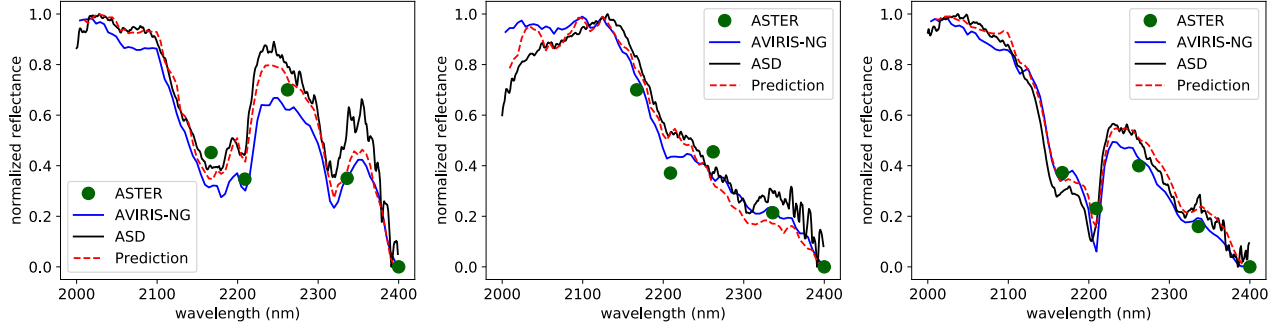


Fig. 8. Examples of spectroscopic measurements from the field experiment at Cuprite, Nevada. These plots correspond to three distinctive minerals in the scene that have also been found on Mars: alunite (left), opal (center), and kaolinite (right).

confirms that entropy is a suitable objective function for spectroscopic mapping.

We then evaluate the performance of the different planners. In all cases, the entropy and reconstruction error show decreasing trends as more samples are collected (Figure 6). It is clear that Random is the worst planner. We compare Greedy (myopic) against MCTS (non-myopic) via a paired t-test (Figure 7). Results indicate that MCTS is not necessarily better at the beginning, but it outperforms Greedy in the long term. Overall, we confirm that algorithms with farther planning horizons tend to perform better.

VII. FIELD EXPERIMENTS

A. Experimental Setup

We performed a set of autonomous rover traverses in the field in order to validate the simulation results. The rover platform that was used is Zoë (Figure 1) [15]. It carried a computer with an Intel i7 processor with a base frequency of 2.8 GHz and 4 cores, as well as 4GB of DDR4 memory. In general, computation time was not an issue. Depending on the complexity of each path planner, the planning process for each waypoint took just a few seconds or minutes to run.

The rover carried an ASD FieldSpec Pro spectrometer with a 1° foreoptic mounted on a pan-tilt mechanism. Each measurement consisted in a *panorama* that acquired and averaged 16 spectra, moving the pan-tilt actuator in a 5×5 m raster pattern. The spectrometer was calibrated for each panorama using an onboard white reference. Panoramas were monitored both automatically and manually; whenever faulty (e.g. there was a shadow on the calibration target), they were recalibrated and retaken. The ASD spectra were interpolated and downsampled so they would have the same resolution as AVIRIS-NG. This was done in order to use the same models from the simulated experiment.

Zoë used GPS localization to save its geographic coordinates whenever it collected an ASD panorama. Zoë used a planar homography to convert from geographic coordinates (latitude and longitude) to map pixel coordinates (row and column), enabling the spatial registration of *in situ* and remote spectra, respectively. Inherent GPS error was negligible since the used spectroscopic maps have a resolution of 15

m/pixel. The rover considered that it had reached a waypoint whenever it was less than 5 m away from it.

Safe rover navigation was one of the main challenges we faced. The terrain was not always traversable at Cuprite. As in the simulations, we used the ASTER DEM to try to enforce a slope constraint of 18° . It proved somewhat useful, but not sufficient because of the poor DEM resolution (15 m/pixel). Human supervision and manual overriding were occasionally required for risk and obstacle avoidance.

As opposed to the simulation studies, Zoë was unable to execute hundreds of traverses; instead, it generated and traversed three paths, each one running a different planner. This process was repeated at three different sites.

B. Results

We first compare a few ASD spectra that were collected by Zoë at Cuprite against the ASTER and AVIRIS-NG measurements that correspond to the same geographic coordinates (Figure 8). The ASD and AVIRIS-NG spectra align well, showing that the latter is an adequate validation source. This figure also shows the *maximum a posteriori* predictions of the model, which are not only accurate, but also remove some of the noise in the ASD measurements.

The rover traverses at one site at Cuprite are illustrated in Figure 9, along with their respective entropy and reconstruction error plots. The plots are not as smooth as the ones from the simulations because they correspond to a single trial. While entropy is monotonic, this is not always true for reconstruction error. Reasons include *in situ* measurement noise, slight underfitting or overfitting of the model, and small differences between ASD and AVIRIS-NG spectra (Figure 8). Nevertheless, both entropy and error show a decreasing trend. We observe that the non-myopic MCTS planner has the best performance overall.

Finally, we demonstrate the active learning process during a traverse from the MCTS planner. Figures 10 and 11 show the entropy throughout the map, as well as 95% confidence prediction intervals for two unsampled locations, which were approximated via Monte Carlo sampling. At first, when just one sample has been collected (Figure 10), the performance of the spatio-spectral regression is poor and there is large uncertainty in the spectroscopic map, especially in places

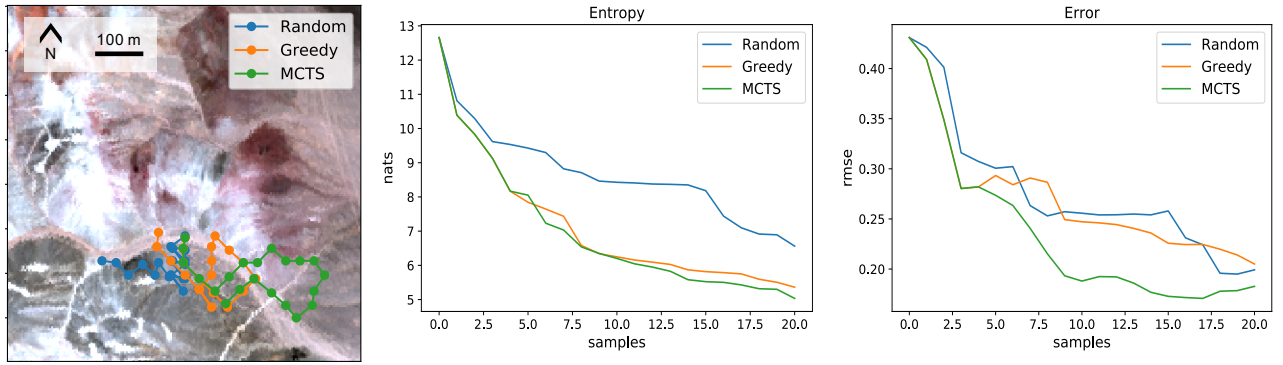


Fig. 9. Results from the field experiment with the rover Zoë at Cuprite: traversed paths (left), entropy (center) and reconstruction error (right) plots.

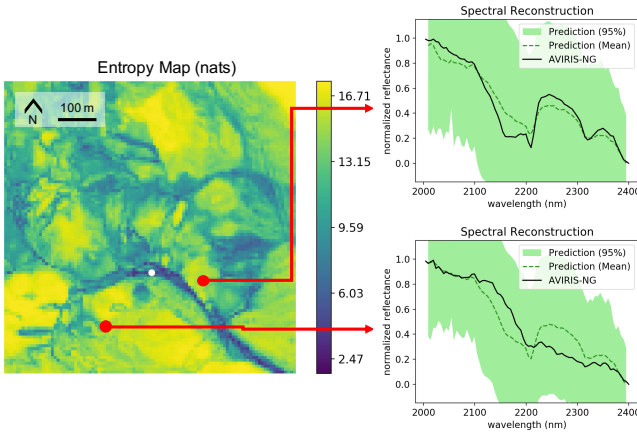


Fig. 10. Active spectroscopic map at Cuprite after collecting one *in situ* sample. Predictions are poor and uncertainty is high.

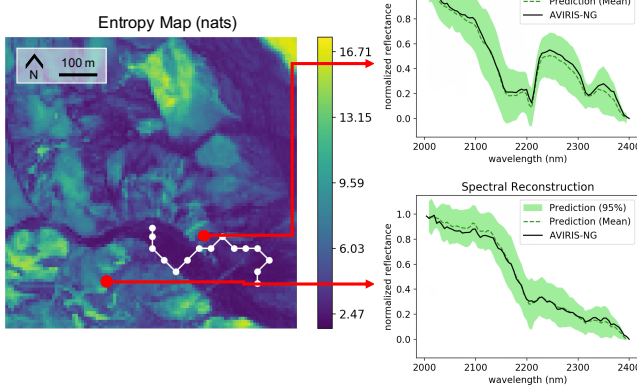


Fig. 11. Active spectroscopic map at Cuprite after collecting multiple *in situ* samples. Predictions improve and uncertainty reduces.

that are significantly different to the sampled locations. MCTS, a non-myopic planner, attempts to collect the most representative samples. After the rover has collected diverse samples (Figure 11), the model's predictions resemble the AVIRIS-NG ground truth, even at unsampled locations, and entropy decreases substantially throughout the map.

VIII. CONCLUSIONS

This paper presents an active learning model for autonomous mapping in planetary rover exploration. It synergistically combines *remote* (orbital) and *in situ* (rover) measurements in order to map and reconstruct the spectroscopic map of an explored scene. This is done by fusing feature extraction and Gaussian process regression to successfully perform multivariate spatial regression. Furthermore, exploration and productivity are improved by incorporating notions from information theory and non-myopic path planning.

Our simulation studies revealed important things. Entropy and reconstruction error are strongly correlated, showing that entropy is a suitable objective function for scene mapping in this scenario. We also confirm that non-myopic planning consistently outperforms simpler exploration strategies such as myopic planning and random sampling.

The results from the field experiment with the rover Zoë demonstrate the viability of our approach in a real exploration scenario using a robotic platform. Important lessons were learned, especially those related to processes that tend to be oversimplified in simulations, such *in situ* measurement collection and safe terrain navigation.

Future investigations will improve and expand the spatio-spectral regression model; examples include explicit mineral classifications and the incorporation of prior domain knowledge. They will also address the trade-off between safe traversability and science productivity in heterogeneous terrains. Finally, we will apply these methods to other scientific endeavors that could also benefit from autonomous robotic exploration, such as maritime or agricultural mapping.

ACKNOWLEDGMENT

This research was supported by the National Science Foundation National Robotics Initiative Grant #IIS-1526667. We acknowledge support of the NASA Earth Science Division for the use of AVIRIS-NG data. A portion of this work was carried out at the Jet Propulsion Laboratory, California Institute of Technology, under a contract with the National Aeronautics and Space Administration. Copyright 2020, All Rights Reserved. U.S. government support acknowledged.

REFERENCES

- [1] D. Gaines, G. Doran, H. Justice, G. Rabideau, S. Schaffer, V. Verma, K. Wagstaff, A. Vasavada, W. Huffman, R. Anderson, R. Mackey, and T. Estlin, "Productivity Challenges for Mars Rover Operations: A Case Study of Mars Science Laboratory Operations Executive Summary," Jet Propulsion Laboratory, Tech. Rep. Technical Report D-97908, 2016. [Online]. Available: https://ai.jpl.nasa.gov/public/papers/gaines_report_roverProductivity.pdf
- [2] D. Gaines, J. Russino, G. Doran, R. Mackey, M. Paton, B. Rothrock, S. Schaffer, A.-A. Agha-Mohammadi, C. Joswig, H. Justice, K. Kolcio, J. Sawoniewicz, V. Wong, K. Yu, G. Rabideau, R. Anderson, and A. Vasavada, "Self-Reliant Rover Design for Increasing Mission Productivity," in *International Symposium on Artificial Intelligence, Robotics and Automation in Space (i-SAIRAS)*, 2018. [Online]. Available: https://ai.jpl.nasa.gov/public/papers/gaines_planrob2018.reliant.pdf
- [3] R. W. Zurek and S. E. Smrekar, "An overview of the Mars Reconnaissance Orbiter (MRO) science mission," *Journal of Geophysical Research E: Planets*, vol. 112, no. 5, pp. 1–22, 2007.
- [4] S. L. Mouélic, J. P. Combe, V. Sarago, N. Mangold, M. Massé, J. P. Bibring, B. Gondet, Y. Langevin, and C. Sotin, "An iterative least squares approach to decorrelate minerals and ices contributions in hyperspectral images: Application to Cuprite (earth) and Mars," in *2009 First Workshop on Hyperspectral Image and Signal Processing: Evolution in Remote Sensing*, 2009, pp. 1–4.
- [5] C. E. Viviano-Beck, F. P. Seelos, S. L. Murchie, E. G. Kahn, K. D. Seelos, H. W. Taylor, K. Taylor, B. L. Ehlmann, S. M. Wiseman, J. F. Mustard, and M. F. Morgan, "Revised crism spectral parameters and summary products based on the currently detected mineral diversity on mars," *Journal of Geophysical Research: Planets*, vol. 119, no. 6, pp. 1403–1431, 2014. [Online]. Available: <https://agupubs.onlinelibrary.wiley.com/doi/abs/10.1002/2014JE004627>
- [6] J. L. Bishop, "Chapter 3 - Remote Detection of Phyllosilicates on Mars and Implications for Climate and Habitability," in *From Habitability to Life on Mars*, N. A. Cabrol and E. A. Grin, Eds. Elsevier, 2018, pp. 37 – 75. [Online]. Available: <http://www.sciencedirect.com/science/article/pii/B9780128099353000037>
- [7] T. M. Cover and J. A. Thomas, *Elements of Information Theory*, 2nd ed. Hoboken, NJ: Wiley- Interscience, 2006.
- [8] D. R. Thompson, "Intelligent mapping for autonomous robotic survey," Ph.D. dissertation, Carnegie Mellon University, Pittsburgh, PA, August 2008.
- [9] A. Candela, D. Thompson, E. N. Dobrea, and D. Wettergreen, "Planetary robotic exploration driven by science hypotheses for geologic mapping," in *2017 IEEE/RSJ International Conference on Intelligent Robots and Systems (IROS)*, Sep. 2017, pp. 3811–3818.
- [10] A. Krause, A. P. Singh, and C. Guestrin, "Near-Optimal Sensor Placements in Gaussian Processes: Theory, Efficient Algorithms and Empirical Studies," *Journal of Machine Learning Research*, vol. 9, pp. 235–284, 2008. [Online]. Available: <http://portal.acm.org/citation.cfm?doid=1102351.1102385>
- [11] J. Binney and G. S. Sukhatme, "Branch and bound for informative path planning," in *2012 IEEE International Conference on Robotics and Automation*, May 2012, pp. 2147–2154.
- [12] S. Kodgule, A. Candela, and D. Wettergreen, "Non-myopic planetary exploration combining in situ and remote measurements," in *2019 IEEE/RSJ International Conference on Intelligent Robots and Systems (IROS)*, Nov 2019, pp. 536–543.
- [13] G. A. Swayze, R. N. Clark, A. F. H. Goetz, K. E. Livo, G. N. Breit, F. A. Kruse, S. J. Sutley, L. W. Snee, H. A. Lowers, J. L. Post, R. E. Stoffregen, and R. P. Ashley, "Mapping Advanced Argillite Alteration at Cuprite, Nevada, Using Imaging Spectroscopy," *Economic Geology*, vol. 109, no. 5, pp. 1179–1221, 2014.
- [14] D. R. Thompson, A. Candela, D. S. Wettergreen, E. Noe Dobrea, G. A. Swayze, R. N. Clark, and R. Greenberger, "Spatial Spectroscopic Models for Remote Exploration," *Astrobiology*, vol. 18, no. 7, pp. 934–954, 2018.
- [15] D. Wettergreen, N. Cabrol, V. Baskaran, F. Calderón, S. Heys, D. Jonak, A. Luders, D. Pane, T. Smith, J. Teza, P. Tompkins, D. Villa, C. Williams, and M. Wagner, "Second Experiments in the Robotic Investigation of Life in the Atacama Desert of Chile," in *International Symposium on Artificial Intelligence, Robotics and Automation in Space (i-SAIRAS)*, 2005.
- [16] G. Foil, D. R. Thompson, W. Abbey, and D. S. Wettergreen, "Probabilistic surface classification for rover instrument targeting," in *2013 IEEE/RSJ International Conference on Intelligent Robots and Systems*, Nov 2013, pp. 775–782.
- [17] L. Pedersen, M. Wagner, D. Apostolopoulos, and W. R. Whittaker, "Autonomous robotic meteorite identification in antarctica," in *Proceedings 2001 ICRA. IEEE International Conference on Robotics and Automation (Cat. No.01CH37164)*, vol. 4, May 2001, pp. 4158–4165 vol.4.
- [18] M. Gallant, A. Ellery, and J. Marshall, "Science-influenced mobile robot guidance using Bayesian Networks," in *Canadian Conference on Electrical and Computer Engineering*. IEEE, 2011, pp. 1135–1139.
- [19] T. A. Estlin, B. J. Bornstein, D. M. Gaines, R. C. Anderson, D. R. Thompson, M. Burl, R. Castaño, and M. Judd, "Aegis automated science targeting for the mer opportunity rover," *ACM Transactions on Intelligent Systems and Technology (TIST)*, vol. 3, no. 3, May 2012. [Online]. Available: <https://doi.org/10.1145/2168752.2168764>
- [20] J. Binney, A. Krause, and G. S. Sukhatme, "Informative path planning for an autonomous underwater vehicle," in *2010 IEEE International Conference on Robotics and Automation*, May 2010, pp. 4791–4796.
- [21] M. Woods, A. Shaw, D. Barnes, D. Price, D. Long, and D. Pullan, "Autonomous science for an exomars rover-like mission," *Journal of Field Robotics*, vol. 26, no. 4, pp. 358–390, 2009. [Online]. Available: <http://dx.doi.org/10.1002/rob.20289>
- [22] S. Chien, R. Sherwood, D. Tran, B. Cichy, G. Rabideau, R. Castano, A. Davis, and D. Boyer, "Using autonomy flight software to improve science return on earth observing one," *Journal of Aerospace Computing, Information, and Communication*, vol. 2, pp. 196–216, 2005.
- [23] A. Castano, A. Fukunaga, J. Biesiadecki, L. Neakrase, P. Whelley, R. Greeley, M. Lemmon, R. Castano, and S. Chien, "Autonomous detection of dust devils and clouds on mars," in *2006 International Conference on Image Processing*, Oct 2006, pp. 2765–2768.
- [24] S. Kumar, W. Luo, G. Kantor, and K. Sycara, "Active Learning with Gaussian Processes for High Throughput Phenotyping," in *Proceedings of the 18th International Conference on Autonomous Agents and MultiAgent Systems*. Montreal QC, Canada: International Foundation for Autonomous Agents and Multiagent Systems, 2019, pp. 2078—2080. [Online]. Available: <http://dl.acm.org/citation.cfm?id=3306127.3332016>
- [25] A. Arora, R. Fitch, and S. Sukkarieh, "An approach to autonomous science by modeling geological knowledge in a bayesian framework," in *2017 IEEE/RSJ International Conference on Intelligent Robots and Systems (IROS)*, Sep. 2017, pp. 3803–3810.
- [26] D. R. Thompson, D. Wettergreen, G. Foil, M. Furlong, and A. R. Kiran, "Spatio-spectral exploration combining in situ and remote measurements," in *Twenty-Ninth AAAI Conference on Artificial Intelligence*, 2015, pp. 3679–3685.
- [27] A. Candela, D. R. Thompson, and D. Wettergreen, "Automatic Experimental Design Using Deep Generative Models Of Orbital Data," in *International Symposium on Artificial Intelligence, Robotics and Automation in Space (i-SAIRAS)*, 2018.
- [28] G. Foil and D. Wettergreen, "Efficiently sampling from underlying models," in *Proceedings of Robotics: Science and Systems*, Pittsburgh, Pennsylvania, June 2018.
- [29] R. N. Clark, "Spectroscopy of rocks and minerals, and principles of spectroscopy," *Manual of Remote Sensing*, vol. 3, pp. 3–58, 1999.
- [30] N. A. Cressie, *Statistics for Spatial Data*. John Wiley & Sons, Inc., 1993.
- [31] D. P. Kingma and M. Welling, "Auto-Encoding Variational Bayes," *arXiv preprint arXiv:1312.6114*, 2013. [Online]. Available: <http://arxiv.org/abs/1312.6114>
- [32] D. J. Rezende, S. Mohamed, and D. Wierstra, "Stochastic Backpropagation and Approximate Inference in Deep Generative Models," in *Proceedings of the 31st International Conference on Machine Learning (ICML)*, vol. 32, no. 2, 2014, pp. 1278—1286. [Online]. Available: <http://arxiv.org/abs/1401.4082>
- [33] C. E. Rasmussen and C. K. I. Williams, *Gaussian Processes for Machine Learning*. Cambridge, Massachusetts: The MIT Press, 2006. [Online]. Available: www.GaussianProcess.org/gpml
- [34] S. Thrun, W. Burgard, and D. Fox, *Probabilistic Robotics*, 1st ed. Cambridge, Massachusetts: The MIT Press, 2005.
- [35] C. Chekuri and M. Pal, "A recursive greedy algorithm for walks in directed graphs," in *Proceedings of the 46th Annual IEEE Symposium on Foundations of Computer Science*, ser. FOCS '05. Washington,

- DC, USA: IEEE Computer Society, 2005, pp. 245–253. [Online]. Available: <http://dx.doi.org/10.1109/SFCS.2005.9>
- [36] N. K. Yilmaz, C. Evangelinos, P. F. J. Lermusiaux, and N. M. Patrikalakis, “Path planning of autonomous underwater vehicles for adaptive sampling using mixed integer linear programming,” *IEEE Journal of Oceanic Engineering*, vol. 33, no. 4, pp. 522–537, Oct 2008.
- [37] G. A. Hollinger and G. S. Sukhatme, “Sampling-based robotic information gathering algorithms,” *The International Journal of Robotics Research*, vol. 33, no. 9, pp. 1271–1287, 2014. [Online]. Available: <http://dx.doi.org/10.1177/0278364914533443>
- [38] H. Fujisada, F. Sakuma, A. Ono, and M. Kudoh, “Design and preflight performance of aster instrument prototypical model,” *IEEE Transactions on Geoscience and Remote Sensing*, vol. 36, no. 4, pp. 1152–1160, 1998.
- [39] L. Hamlin, R. O. Green, P. Mourolis, M. Eastwood, D. Wilson, M. Dudik, and C. Paine, “Imaging spectrometer science measurements for terrestrial ecology: AVIRIS and new developments,” *IEEE Aerospace Conference Proceedings*, pp. 1–7, 2011.